

Elastomeric waveguide on-chip coupling of an encapsulated MoS₂ monolayer

Filip Auksztol,^{*,†} Daniele Vella,[‡] Ivan Verzhbitskiy,[‡] Kian Fong Ng,[†] Yi Wei Ho,^{¶,§,‡} James A. Grieve,[†] José Viana-Gomes,^{‡,§} Goki Eda,^{‡,||,§} and Alexander Ling^{*,†,‡}

[†]*Centre for Quantum Technologies, National University of Singapore*

[‡]*Department of Physics, National University of Singapore*

[¶]*NUS Graduate School for Integrative Sciences and Engineering*

[§]*Centre for Advanced 2D Materials and Graphene Research Centre*

^{||}*Department of Chemistry, National University of Singapore*

E-mail: oxon@nus.edu.sg; cqtalej@nus.edu.sg

Abstract

We propose a robust photonic platform for encapsulation and addressing of optically active 2D- and nano-materials. Our implementation utilises a monolayer of MoS₂ transition metal dichalcogenide embedded in an elastomeric waveguide chip. The structure is manufactured from PDMS using soft-lithography and capable of sustaining a single mode of guided light. We prove that this setup facilitates addressing of the 2D material flake by pumping it with polarised laser light and gathering polarisation-resolved photoluminescence spectra with the extinction ratio of 31, which highlights the potential for selection-rule dependent measurements. Our results demonstrate improved handling of the material and experimental simplification compared to other techniques.

Furthermore, inherent elasticity of the host provides an avenue for direct mechanical coupling to embedded materials.

Advances in the fundamental understanding of ultra-thin transition metal dichalcogenides (TMDs) including their excitonic properties,¹ exciton-phonon coupling,² optical selection rules³ and valley degree of freedom,⁴ position them as attractive candidates for components of devices in novel photonic and optoelectronic applications.⁵⁻⁸ Monolayer materials are fragile and difficult to handle due to the micrometer footprint and their tendency to crumple. In order to incorporate them in the existing photonic systems, there is a need for packaging in the form of a robust platform for handling and testing of the material. Planar photonic waveguide chips capable of confining light on the micrometer scale are a natural candidate for such a platform, offering transmission of visible light, polarisation selectivity and shielding from environmental influence. While this is challenging to achieve with traditional semiconductor or glass waveguide structures, we propose that a photonic device fabricated in an elastomer can serve as a host for encapsulation of the monolayers and their heterostructures. Using the suggested geometry, we show it is feasible to confine an optically active 2D material within the mode of guided light, allowing for the propagation of linearly polarised light in the plane of the monolayer. As reported previously⁹ such waveguides are capable of guiding orthogonal polarization states with very similar mode profiles. This allows the polarisation of light in this system to be changed such that exciton states with different optical selection rules (e.g. dark and bright excitons) can be independently accessed. Embedding the material of interest in an elastomer gives an added benefit of direct mechanical coupling by performing either global or local deformation of the chip.

Here, we describe a proof-of-concept device, utilising a monolayer of MoS₂ encapsulated within the mode of light guided in a polydimethylsiloxane (PDMS) chip. A stylised illustration of the experimental sample (Figure 1a) shows an MoS₂ flake inserted between the two layers of PDMS. Different refractive indices of the layers (1.4320 and 1.4311, simulated), together with the geometry of the top ridge, create a light-guiding structure capable of sus-

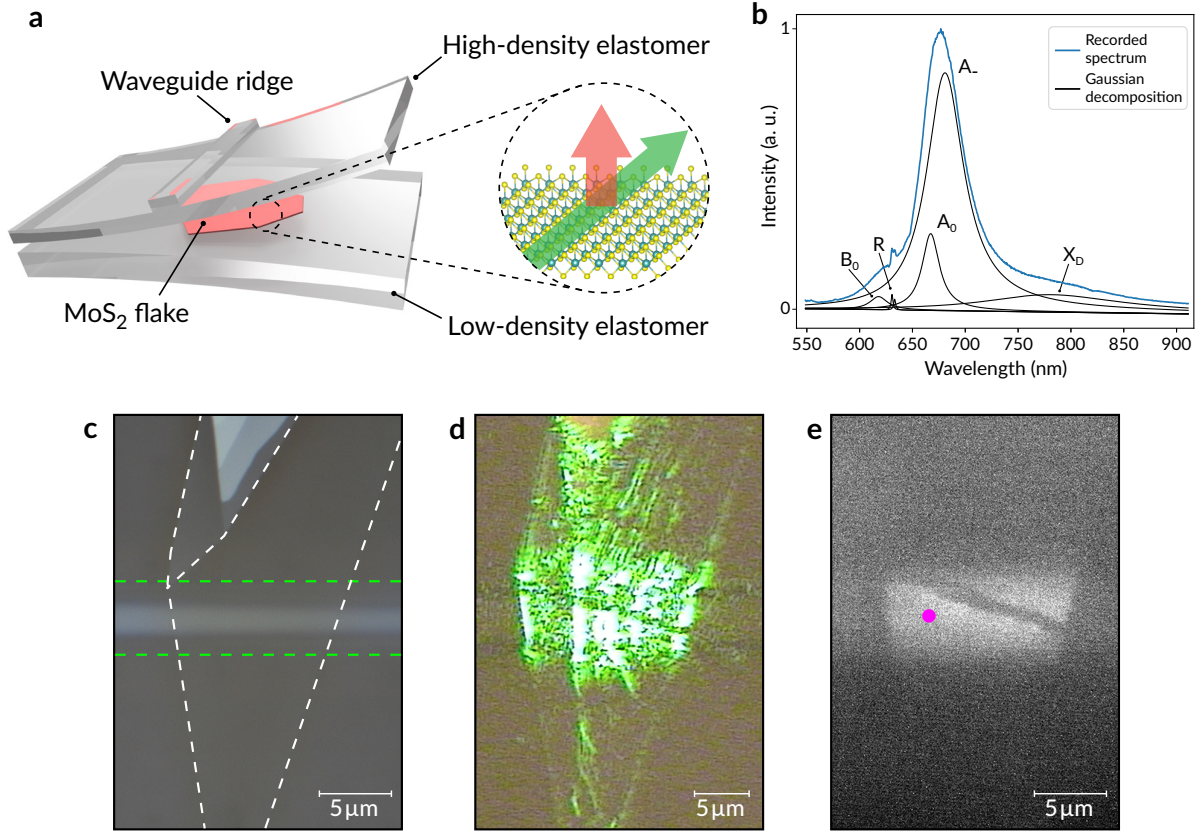


Figure 1: Elastomeric waveguide structure with optically active material encapsulated within the guided mode of light. (a) Artistic representation of the monolayer of MoS_2 encapsulated within the waveguide structure comprised of two layers of elastomer with different densities. Call-out shows the schematic representation of addressing (green arrow) and collection (red arrow) geometry with respect to the MoS_2 monolayer. (b) Waveguide excitation photoluminescence spectrum collected from the encapsulated MoS_2 monolayer. Physical origins of the individual components of the spectrum are deduced by fitting the Gaussian functions, which correspond to: neutral B-exciton (B_0), substrate Raman doublet (R), neutral A-exciton (A_0), charged A-exciton (A_-), defect emission (X_D). (c) Optical microscope image ($\times 100$ magnification) of the encapsulated flake. White dashed lines outline the flake and the boundary between the monolayer and bulk material. Green dashed lines outline the edges of the waveguide ($5\ \mu\text{m}$ width). (d) Flake illuminated with 532 nm pump delivered to the sample via the waveguide. (e) Optical microscope image of the PL emission during the waveguide excitation of the sample. Pump is blocked with a long-pass filter. Magenta dot indicates the probing region, from which the PL spectrum has been collected during the polarisation dependence experiment.

taining a single mode of radiation (see inset in Figure 2 for an image of the guided mode). Positioning a flake of 2D material within the mode of the guided light allows for efficient coupling. Here, we demonstrate this experimentally for a flake of MoS₂ by exciting it through the waveguide and performing room temperature measurement of the photoluminescence spectrum while varying the polarisation of incident light.

Experiment

The experimental setup for the excitation and collection of PL spectra is shown in Figure 2. 532 nm laser light is coupled to a single-mode fibre, which is cut and stripped at one end to expose the core and cladding. The exposed end is mounted on a micrometre stage (Newport ULTRAlign XYZ + yaw, pitch, roll) and aligned to couple to the chip waveguide that encapsulates the MoS₂ flake. Coupling is optimised by maximising the transmitted power collected by the imaging objective on the opposite end of the chip ($\times 20$). The incident light couples to the MoS₂ monolayer and the resulting photoluminescence is collected by a high NA top-down objective ($\times 100$), after passing through the long-pass filter to eliminate the excitation wavelength. To achieve linear polarization at the location of the MoS₂ flake, strain-induced birefringence in the single mode fibre (and to a lesser extent the waveguide itself) is pre-compensated using a quarter wave plate and half wave plate. Once completed, the polarization of the excitation beam at the location of the flake can be rotated in the linear basis by additional rotation of the half wave plate alone.

Results

The encapsulated flake is investigated in detail by spatial mapping of the photoluminescence spectrum by normal excitation, which shows the distribution of the integrated photoluminescence, linewidth broadening and the peak position for the 620–720 nm spectral range (Figures 3a, b and c respectively). Figure 3a reveals the integrated photoluminescence spectrum map for the area of the flake within and around the edges of the waveguide ridge, with

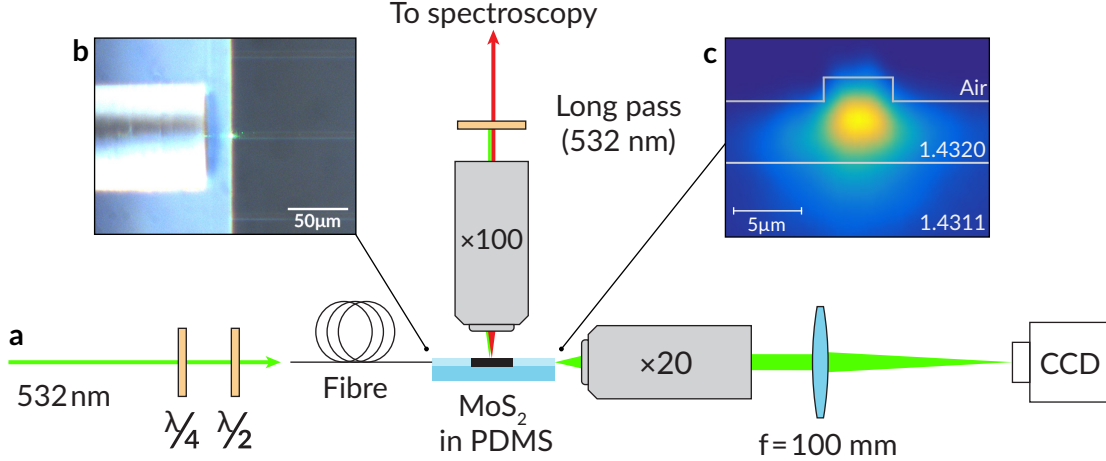


Figure 2: (a) Photoluminescence experimental setup (chip side-view perspective). Exposed fibre tip, the waveguide chip and the imaging microscope are each mounted independently on micrometre stages for alignment. The top-down microscope is part of a larger spectroscopy setup (custom-designed NTEGRA system by NT-MDT). (b) Microscope image of the fibre tip coupling 532 nm pump laser to the waveguide chip. 125 μm diameter cladding of the fibre is visible, together with three 5 μm waveguides on the chip. (c) Experimental TEM mode of the transmitted light, measured at the end-face of the waveguide chip (see arrow).

variations that can be attributed to the spatial inhomogeneity of the flake. This is likely due to wrinkles formed during the fabrication of the low-density elastomer layer of the waveguide. There is a correlation between the linewidth distribution and the photoluminescence intensity (compare Figure 3a and b), with narrow emission implying high area and intensity.

The map of the peak distribution (Figure 3c) shows a strong correlation with the waveguide geometry, with the two regions of interest separated by the edges of the waveguide ridge. The photoluminescence peak undergoes a red shift of ~ 17 nm between the outer region towards the waveguide ridge. Figure 3d shows extracted photoluminescence spectra from different regions of the monolayer flake. Such spectrum mainly consists of the ground exciton peak¹⁰ originating from the direct optical transition at the K and K' points of the Brillouin zone.^{11,12} The strong asymmetric photoluminescence peak is made of two contributions: neutral (A_0) and charged (A_-) excitons^{13,14} separated by 45 meV (See Fig. 1b). Noticeably, relative intensities of these two peaks vary spatially, resulting in the apparent

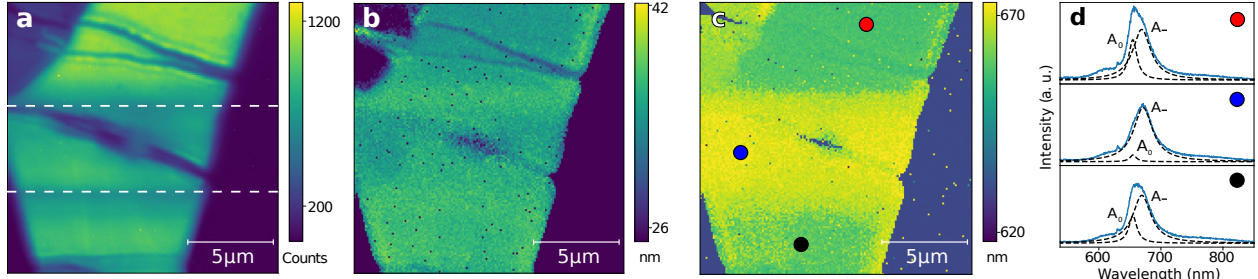


Figure 3: Photoluminescence maps of the flake area obtained with NTEGRA (NT-MDT) piezo-controlled spectrometer. (a) Integrated photoluminescence in the vicinity of the waveguide ridge. White dashed lines indicate edges of the waveguide. Irregularities in the monolayer are visible in the waveguide path. (b) Linewidth broadening. (c) Peak position showing a strong correlation with waveguide geometry. (d) Sample spectra obtained from the approximate positions marked in (c). See text for explanation.

changes of the cumulative line-shape. Similar modifications of the optical properties have been reported for uniaxially² and biaxially¹⁵ strained monolayer of MoS₂.

Subsequently, we study the polarisation dependence of the photoluminescence spectra, which are obtained by parallel excitation of the flake with incident pump light delivered to the material through the waveguide (see call-out in Figure 1a). A monolayer of MoS₂ is pumped with in-plane 532 nm laser light to induce the primary photoexcitations (excitons) (Figure 4a). The resultant photoluminescence spectrum is collected from the probing region (Figure 1e) and reveals the typical characteristics of monolayer MoS₂.

Polarisation parallel to the flake surface produced maximum excitation (photoluminescence) and conversely, orthogonal polarisation minimised the excitation (see Figure 4a for comparison of intensities). This is in agreement with the two-dimensional nature of the bright excitons, that offer maximum cross section for polarisation of light when it is parallel to the flake.¹⁶ By rotating the polarisation of the incident light, the excitonic emission is not completely extinguished. Assuming the finite theoretical limit of the extinction, we speculate it is further reduced due to the irregularities in the monolayer surface (introduced during the dry-stamping transfer process), which act as scattering centres, visible in Figure 1d. Similar photoluminescence curves are recorded for intermediate values of polarisation in the increments of 10°. The resultant spectra are integrated, normalised for power (to mit-

igate the laser instabilities) and plotted against the polarisation angle (Figure 4b). Power for the normalisation is recorded after passing through the chip, at the position of a CCD sensor (Figure 2). The normalised points are then fitted to a sine function that demonstrates the polarisation dependence of photoluminescence with high extinction ratio of 31 between parallel and perpendicular states, which compares favourably with previous reports.¹⁷

In addition, we have performed measurements of photoluminescence at the end face of the chip comparing two identical waveguides, one of which contained the flake. The flake generates bright exciton emission at a normal to its plane, which does not couple back into the guided mode and we have indeed observed no resolvable photoluminescence signal at the output of the waveguide. Further to this, we aim to extend the experiment to investigate emission of the dark exciton in MoS₂ and other dichalcogenide monolayers,^{1,3} which has the potential for waveguide out-coupling in our geometry.

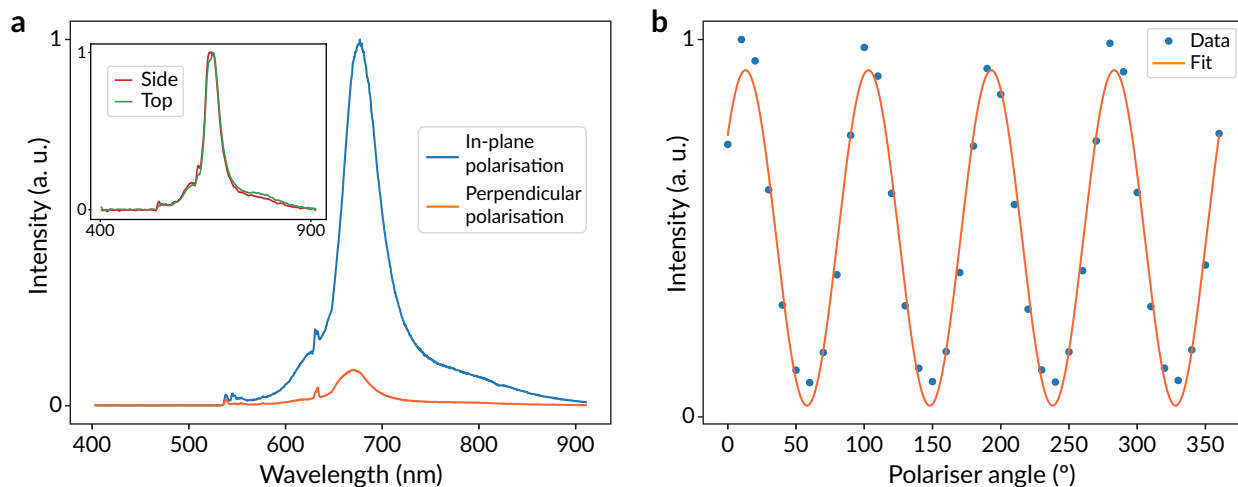


Figure 4: Photoluminescence measurement with 532 nm pump. (a) Photoluminescence spectra of encapsulated MoS₂ flake excited through the waveguide with incident in-plane polarisation (blue) and perpendicular polarisation (orange). Inset shows normalized spectra with top and side (through the waveguide with in-plane polarisation) excitation. (b) Photoluminescence spectra for intermediate polarisation states, integrated and normalised for power (blue) with sine function fit (orange). Extinction ratio of fitted function is 31 with oscillation period of 90.0° (which corresponds to an 180.0° rotation period of the polarisation).

Conclusion

We have presented a working prototype of a photonic chip with an atomically thin MoS₂ flake, which is encapsulated directly within the single mode of guided laser light. The observed photoluminescence spectra are consistent with the ones present in the literature for monolayers of MoS₂. Sensitivity of the photoluminescence signal to polarisation of pump light is shown, with high extinction ratio and exact expected periodicity of 180°. The chip has shown robustness and ease of handling, being reused in multiple experiments over a period of months without any noticeable degradation in the MoS₂ flake. Such capabilities can enable further experiments dealing with optically active materials, such as 2D monolayers, nano-diamonds, crystalline and organic single photon emitters, and similar.

Methods

The elastomeric waveguide chip is fabricated out of polydimethylsiloxane (PDMS) in a two-step soft lithography process,⁹ with an additional step for material encapsulation. A lithographic mould is prepared by defining 5 µm by 1.6 µm waveguides on a silicon wafer using laser direct-write in the photoresist (AZ1512HS, AZ Electronic Materials). The PDMS liquid precursor is spun onto the mould and cured at 150 °C to create a 5 µm thick high-density layer. The MoS₂ flake is transferred to the cured PDMS layer at the location of a waveguide, using dry-stamping technique.¹⁸ 1 mm of PDMS liquid precursor is then poured on the top of the structure and cured at 70 °C to form a low-density layer and provide a structural base for the chip. The chip is then peeled from the silicon substrate and end-faces are cut using a microtome blade to enable coupling of an optical fibre. Optical microscope images of the encapsulated flake are shown in Figure 1c to e.

MoS₂ was exfoliated from the bulk single-crystal flake (SPI) by the scotch-tape method onto the surface of the clean home-made PDMS slab. The monolayer was identified by contrast, photoluminescence and Raman spectroscopy. Selected flake was then encapsulated in the PDMS waveguide, as explained above.

Funding statement

G.E. acknowledges the Singapore National Research Foundation for funding the research under medium-sized centre programme. G.E. also acknowledges support from the Ministry of Education (MOE), Singapore, under AcRF Tier 2 (MOE2015-T2-2-123, MOE2017-T2-1-134) and AcRF Tier 1 (R-144-000-387-114). A.L., F.A., J.A.G. and K.F.N. acknowledge support from the Ministry of Education (MOE), Singapore under AcRF Tier 3 (MOE2012-T3-1-009) and the National Research Foundation, Prime Ministers Office, Singapore under its Research Centres of Excellence programme.

References

- (1) Robert, C.; Amand, T.; Cadiz, F.; Lagarde, D.; Courtade, E.; Manca, M.; Taniguchi, T.; Watanabe, K.; Urbaszek, B.; Marie, X. Fine structure and lifetime of dark excitons in transition metal dichalcogenide monolayers. *Phys. Rev. B* **2017**, *96*, 155423.
- (2) Niehues, I. et al. Strain Control of ExcitonPhonon Coupling in Atomically Thin Semiconductors. *Nano Lett.* **2018**, *18*, 1751–1757.
- (3) Wang, G.; Robert, C.; Glazov, M. M.; Cadiz, F.; Courtade, E.; Amand, T.; Lagarde, D.; Taniguchi, T.; Watanabe, K.; Urbaszek, B.; Marie, X. In-Plane Propagation of Light in Transition Metal Dichalcogenide Monolayers: Optical Selection Rules. *Phys. Rev. Lett.* **2017**, *119*, 047401.
- (4) Xu, X.; Yao, W.; Xiao, D.; Heinz, T. F. Spin and pseudospins in layered transition metal dichalcogenides. *Nat. Phys.* **2014**, *10*, 343.
- (5) Vella, D.; Ovchinnikov, D.; Martino, N.; Vega-Mayoral, V.; Dumcenco, D.; Kung, Y.-C.; Antognazza, M.-R.; Kis, A.; Lanzani, G.; Mihailovic, D.; Gadermaier, C. Unconventional electroabsorption in monolayer MoS₂. *2D Mater.* **2017**, *4*, 021005.

- (6) Huo, N.; Yang, Y.; Li, J. Optoelectronics based on 2D TMDs and heterostructures. *J. Semicond.* **2017**, *38*, 031002.
- (7) Hill, H. M.; Rigosi, A. F.; Raja, A.; Chernikov, A.; Roquelet, C.; Heinz, T. F. Exciton broadening in WS₂/graphene heterostructures. *Phys. Rev. B* **2017**, *96*, 205401.
- (8) Jiang, J.-W.; Park, H. S. Mechanical properties of MoS₂/graphene heterostructures. *Appl. Phys. Lett.* **2014**, *105*, 033108.
- (9) Grieve, J. A.; Ng, K. F.; Rodrigues, M. J. L. F.; Viana-Gomes, J.; Ling, A. Mechanically tunable integrated beamsplitters on a flexible polymer platform. *Appl. Phys. Lett.* **2017**, *111*, 211106.
- (10) Splendiani, A.; Sun, L.; Zhang, Y.; Li, T.; Kim, J.; Chim, C.-Y.; Galli, G.; Wang, F. Emerging Photoluminescence in Monolayer MoS₂. *Nano Lett.* **2010**, *10*, 1271–1275.
- (11) Mak, K. F.; Lee, C.; Hone, J.; Shan, J.; Heinz, T. F. Atomically Thin MoS₂: A New Direct-Gap Semiconductor. *Phys. Rev. Lett.* **2010**, *105*, 136805.
- (12) Chhowalla, M.; Shin, H.; Eda, G.; Li, L.; Loh, K.; Zhang, H. The chemistry of two-dimensional layered transition metal dichalcogenide nanosheets. *Nat. Chem.* **2013**, *5*, 263.
- (13) Mak, K. F.; He, K.; Lee, C.; Lee, G. H.; Hone, J.; Heinz, T. F.; Shan, J. Tightly bound trions in monolayer MoS₂. *Nat. Mater.* **2013**, *12*, 207–11.
- (14) Chernikov, A.; van der Zande, A. M.; Hill, H. M.; Rigosi, A. F.; Velauthapillai, A.; Hone, J.; Heinz, T. F. Electrical Tuning of Exciton Binding Energies in Monolayer WS₂. *Phys. Rev. Lett.* **2015**, *115*, 126802.
- (15) Lloyd, D.; Liu, X.; Christopher, J. W.; Cantley, L.; Wadehra, A.; Kim, B. L.; Goldberg, B. B.; Swan, A. K.; Bunch, J. S. Band Gap Engineering with Ultralarge Biaxial Strains in Suspended Monolayer MoS₂. *Nano Lett.* **2016**, *16*, 5836–5841.

- (16) Schuller, J. A.; Karaveli, S.; Schiros, T.; He, K.; Yang, S.; Kymissis, I.; Shan, J.; Zia, R. Orientation of luminescent excitons in layered nanomaterials. *Nat. Nanotechnol.* **2013**, *8*, 271.
- (17) Tan, Y.; He, R.; Cheng, C.; Wang, D.; Chen, Y.; Chen, F. Polarization-dependent optical absorption of MoS₂ for refractive index sensing. *Sci. Rep.* **2014**, *4*, 7523.
- (18) Castellanos-Gomez, A.; Buscema, M.; Molenaar, R.; Singh, V.; Janssen, L.; Van der Zant, H. S.; Steele, G. A. Deterministic transfer of two-dimensional materials by all-dry viscoelastic stamping. *2D Mater.* **2014**, *1*, 011002.